Journal of ELECTRONIC MATERIALS, Vol. 46, No. 5, 2017
DOI: 10.1007/s11664-016-5114-0

Thermoelectric Properties of Cl-Doped BiCuSeO Oxyselenides

ZHIFANG ZHOU,[1] XING TAN,[1] GUANGKUN REN,[1] YUANHUA LIN,[1,2] and CEWEN NAN[1]

1.—State Key Laboratory of New Ceramics and Fine Processing, School of Materials Science and Engineering, Tsinghua University, Beijing 100084, People's Republic of China. 2.—e-mail: linyh@tsinghua.edu.cn

BiCuSeO oxyselenide has been reported as a promising thermoelectric material because of its special layered structure. Here, we attempt to synthesize *n*-type BiCuSeO using chlorine to substitute the Se site with the modification of $(Cu_2Se_2)^{2-}$ layers. Our results indicate that Cl doping can influence the electrical and thermal transport properties of BiCuSeO bulk materials. The significant reduction in electrical conductivity (from 40 S cm^{-1} to 10 S cm^{-1}) demonstrates that Cl doping can indeed affect $(Cu_2Se_2)^{2-}$ conducting layers. It may be desirable to obtain *n*-type BiCuSeO by heavy doping of Cl or other elements.

Key words: BiCuSeO, thermoelectric properties, SPS, Cl-doping

INTRODUCTION

Energy and the environment are a major concern worldwide. Thermoelectric (TE) materials are capable of direct conversion of thermal energy to electrical energy, and are widely used in power generation, solid-state cooling and thermal sensors, thus playing an increasingly important role in sustainable development.[1,2] The conversion efficiency for TE materials is depicted by the dimensionless figure of merit ZT, defined as $ZT = \sigma S^2 T/\kappa$, where σ, S, κ and T are electrical conductivity, Seebeck coefficient, thermal conductivity and absolute temperature, respectively.[3] To enhance ZT, two approaches can be employed. The first is by increasing σS^2, which is also referred to as the power factor (PF), and the second is by reducing κ. The PF can be enhanced by band gap engineering,[4] quantum confinement effects[5] and electron energy barrier filtering,[6] while κ cab be reduced through the use of nanostructures[7] and all-scale hierarchical architecture.[8] Compared with alloys such as Bi_2Te_3, PbTe and PbSe, oxide-based materials have the advantages of earth abundance, low cost and non-toxicity. In recent years, several types of oxide ceramics have been widely investigated, including $CaMnO_3$,[9] ZnO[10] and $SrTiO_3$.[11] However, such materials have low ZT values, which are not suitable for commercial applications.

In 2010, the layered oxide-based compound, BiCuSeO, was reported as a promising TE material for its intrinsically low lattice thermal conductivity.[12] BiCuSeO consists of $(Cu_2Se_2)^{2-}$ conducting layers, providing conduction pathways for carriers stacked with $(Bi_2O_2)^{2+}$ insulating layers as a charge reservoir.[13] Although its thermal conductivity is low, its electrical conductivity is too low to obtain a high ZT value. Therefore, efforts have been made to enhance the electrical conductivity, including doping with Ba,[14] Mg,[15] Ca,[16] Pb,[17] and Na[18] at the Bi site, Cu deficiencies,[19] and texturing.[20] *P*-type BiCuSeO materials have been studied for many years, but *n*-type BiCuSeO materials are a new topic. Yang et al.[21] used first-principles calculations to investigate the material's electronic structure and transport properties, and found that the ZT value for *n*-type BiCuSeO increased considerably due to its high electrical conductivity and decreased thermopower. Additionally, few reports have investigated the TE properties of BiCuSeO systems on the substitution of Se sites.

Based on the above considerations, we synthesize the Cl-doped BiCuSeO bulk materials using ball milling and spark plasma sintering (SPS). Our results indicate that Cl elements can be doped into

(Received May 30, 2016; accepted November 1, 2016; published online November 28, 2016)

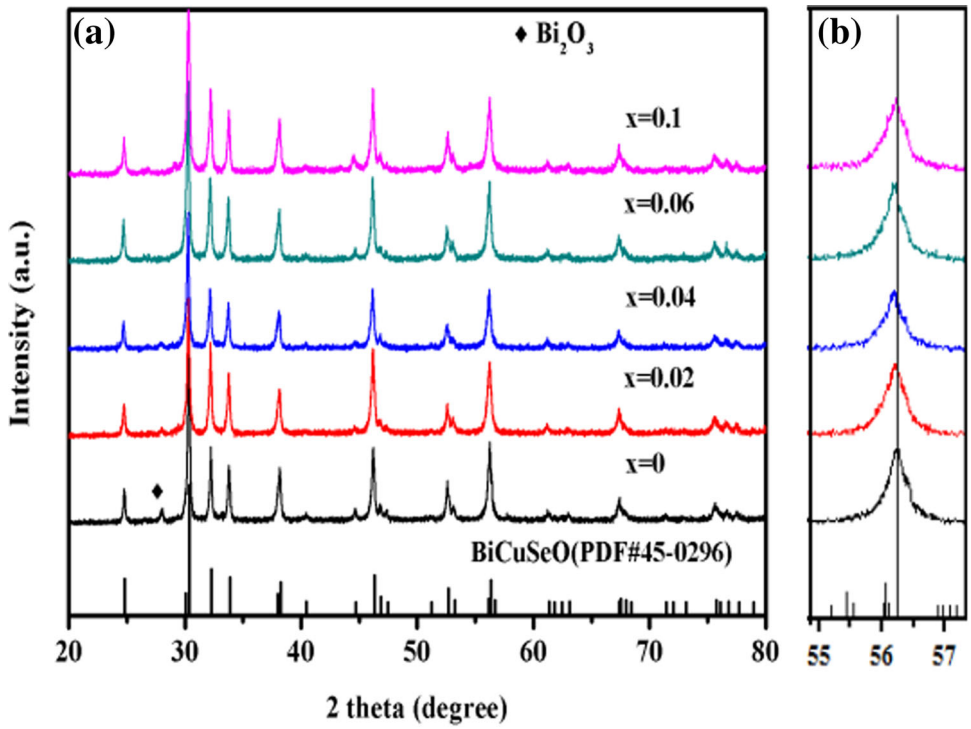

Fig. 1. (a) Bulk XRD patterns for $BiCuSe_{1-x}Cl_xO$. (b) Enlargement patterns between 55° and 57°.

Se sites, which has an obvious influence on the electrical and thermal properties.

EXPERIMENTAL

Sample Preparation

Samples with chemical composition $BiCuSe_{1-x}Cl_xO$ (x = 0, 0.02, 0.04, 0.06, 0.1) were prepared by a two-step solid-state reaction route. The experiments began with the mixing of Bi (4N, Aladdin), Cu (3N, Aladdin), Bi_2O_3 (3N, Aladdin), Se (4N, Aladdin), and BiClO (3N, Alfa Aesar) powders and anhydrous ethanol in a vacuum by ball milling for 4 h at a speed of 350 rpm. The obtained powders were cold-pressed under pressure of 3 MPa into pellets with a diameter of 20 mm, and sealed into evacuated quartz tubes, after which they were heated at 573 K for 5 h and annealed at 973 K for 10 h in a heat treatment furnace. After sintering, samples were crushed into powders in a corundum crucible, followed by ball milling for 8 h. Subsequently, the as-prepared powders were densified by spark plasma sintering (Sumitomo SPS-1050T, Japan) for 5 min at 923 K under axial pressure of 50 MPa.

Characterization

X-ray diffraction (XRD; Bruker D8 ADVANCE A25, Germany) was applied for the phase analysis of $BiCuSe_{1-x}Cl_xO$. The fractured surface morphology of the samples was characterized by field emission scanning electron microscopy (FESEM; JEOL JSM-7001F, Japan). The Seebeck coefficient and electrical conductivity were simultaneously measured using a ZEM-3 instrument (ULVAC-RIKO, Japan) from 300 K to 873 K under a helium atmosphere. Thermal conductivity (κ) was measured indirectly according to the equation $\kappa = DC_P\rho$, where D is thermal diffusivity as measured by the LFA 457 MicroFlash (Netzsch, Germany), ρ is the mass density of samples determined according to the Archimedes method, and C_P is specific heat capacity, which is typically determined by differential scanning calorimetry (DSC), but in this work, the C_P data were was obtained using the Dulong–Petit law. The Hall coefficients were investigated at room temperature and a magnetic field of 1.5 T, from which the carrier concentration and mobility of all samples was able to be determined.

RESULTS AND DISCUSSION

Figure 1a shows the XRD patterns of the bulk $BiCuSe_{1-x}Cl_xO$. All patterns of the sintered samples are consistent with the pure phase of BiCuSeO indexed to the standard Powder Diffraction File (PDF) card 45-0296. A minor peak of Bi_2O_3 was observed in the pure BiCuSeO, which is common in this system and has little effect on the electrical transport properties. Figure 1b shows that the peak between 55° and 57° has no obvious shift with

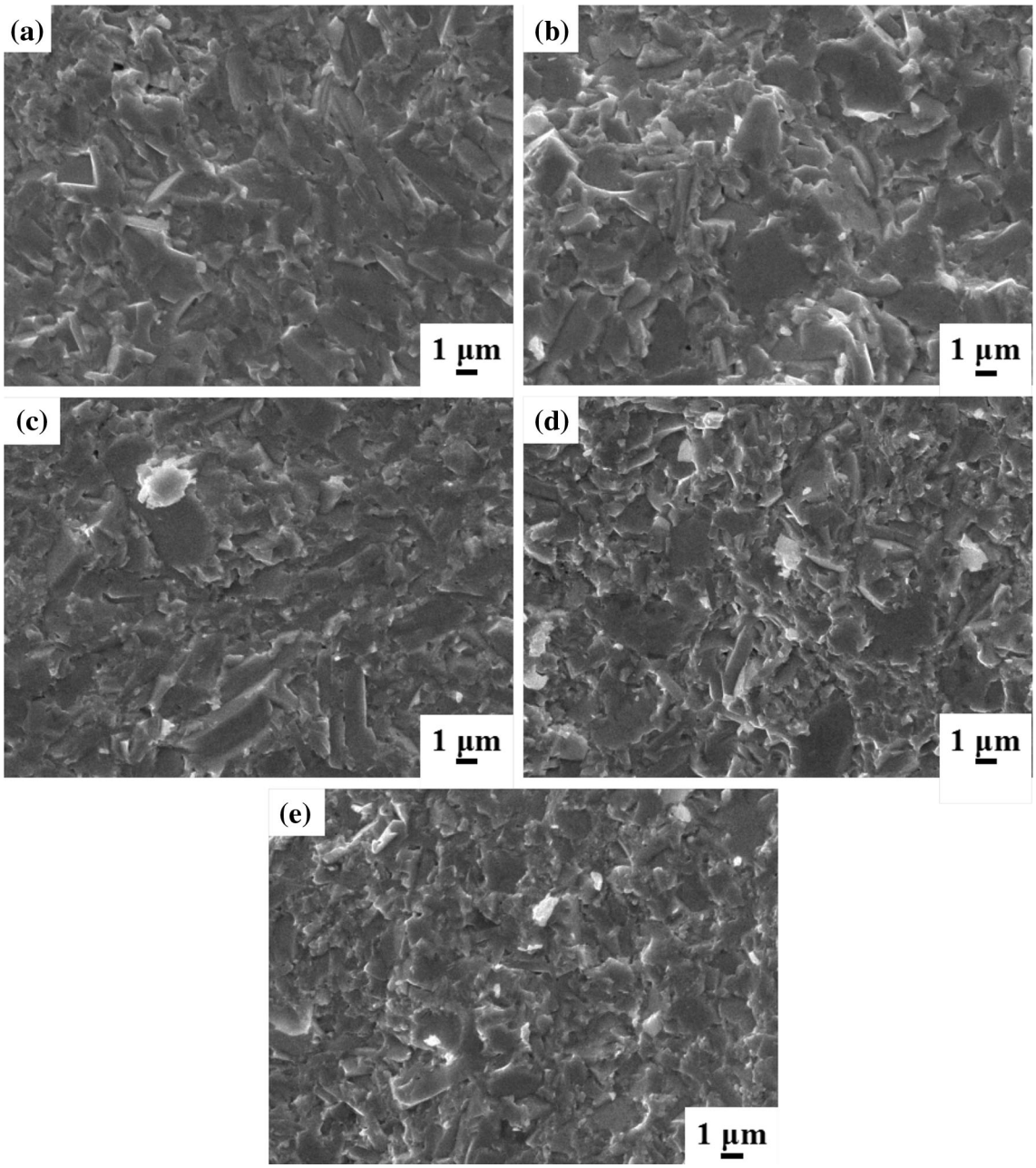

Fig. 2. SEM fractography for $BiCuSe_{1-x}Cl_xO$: (a) $x = 0$, (b) $x = 0.02$, (c) $x = 0.04$, (d) $x = 0.06$, (e) $x = 0.1$.

increasing doping concentration. The radius of Cl^- (0.181 nm) is smaller than that of Se^{2-} (0.198 nm), in which a slight decrease in the lattice parameter should be expected. However, the concentration of holes simultaneously decreases, leading to more anti-bonding states being occupied in the electronic structure. Therefore, the Cu–Se distances become larger, which counterbalances the difference in radius between Cl and Se.

The microstructures of $BiCuSe_{1-x}Cl_xO$ are presented in Fig. 2. After the process of densification by SPS, few pores can be seen in the SEM micrograph, which indicates the high density of all the samples. As the doping concentration of Cl increases, the grain size changes slightly. In Fig. 3, the relative content of Cl in $BiCuSe_{0.98}Cl_{0.02}O$ and $BiCuSe_{0.9}Cl_{0.1}O$ can be seen, with the content of Cl increasing from 0.49% to 2.09% and the content of Se decreasing from 19.66% to 16.06%, which conforms to the doping concentration of Cl. Therefore, this reveals that not only does the actual Cl concentration in the samples increase when the nominal concentration increases, but the concentrations of Cl and Se change in opposite ways with the change in the nominal concentration of Cl.

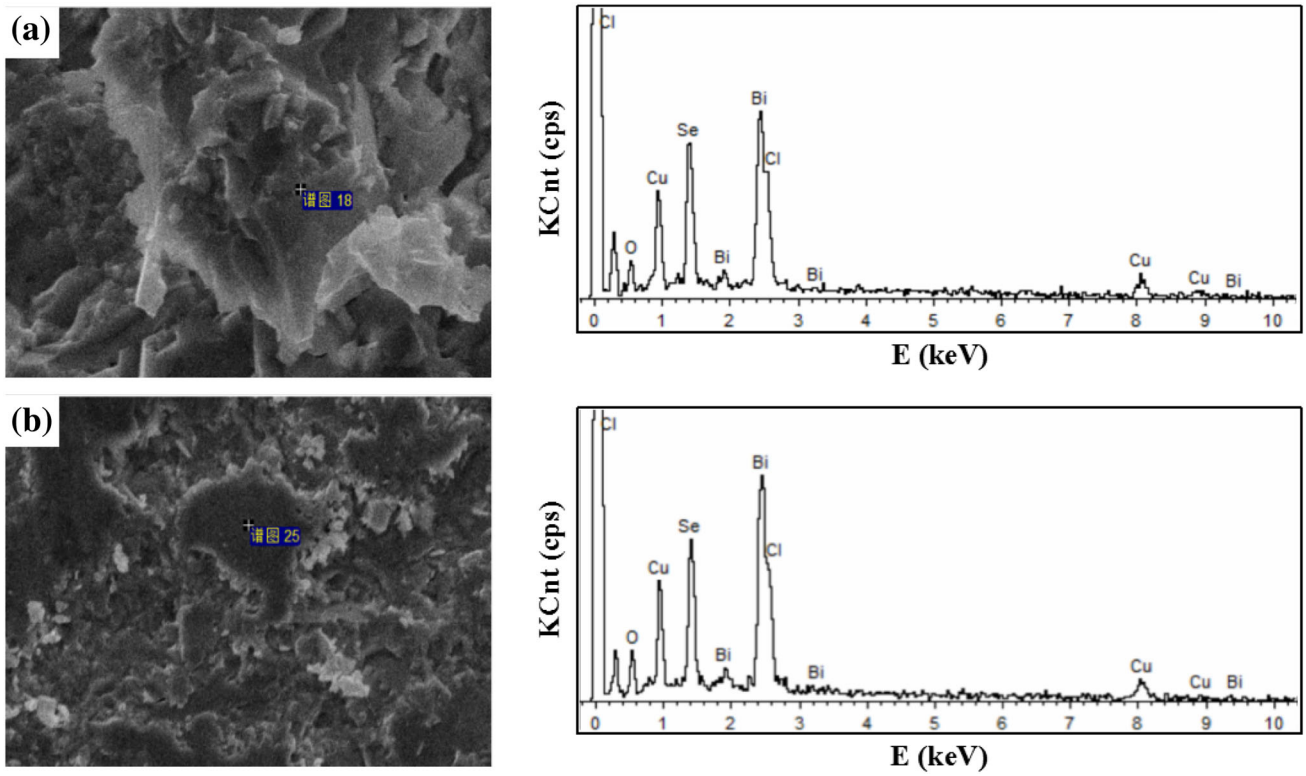

Fig. 3. Energy-dispersive spectroscopy (EDS) for $BiCuSe_{1-x}Cl_xO$: (a) $x = 0.02$, (b) $x = 0.1$.

Figure 4 shows the electrical properties of $BiCuSe_{1-x}Cl_xO$ as a function of temperature, where (a)–(c) are the electrical conductivity, Seebeck coefficient and power factor, respectively. From Fig. 4a, we can see that the electrical conductivity of all samples increases with rising temperature, indicating an intrinsic semiconductor behavior. The pure BiCuSeO has the highest electrical conductivity, reaching 41 S cm^{-1} at 773 K. As the doping concentration increases, the electrical conductivity clearly decreases, which is because Cl serves as an electron donor in *p*-type BiCuSeO in this work. Table I shows the variation in carrier concentration and mobility for $BiCuSe_{1-x}Cl_xO$. The carrier concentration for pure BiCuSeO was approximately 5×10^{18} cm^{-3}, whereas with Cl^- doped into the lattice, the carrier concentration is significantly reduced, indicating that a portion of Se^{2-} was successfully substituted by Cl^-.

From Fig. 4b, we can see that $BiCuSe_{1-x}Cl_xO$ is still a *p*-type semiconductor, because of the positive value of the Seebeck coefficient. The Seebeck coefficient for all samples is relatively high. For $BiCuSe_{0.98}Cl_{0.02}O$, the value reaches 538 $\mu V\ k^{-1}$ at 423 K. Such a high Seebeck coefficient is related to the low carrier concentrations. The PF is calculated by the equation $PF = \sigma S^2$, and the PF of $BiCuSe_{1-x}Cl_xO$ as a function of temperature is shown in Fig. 4c. The variation in PF is very similar to that in Fig. 4a, illustrating that electrical conductivity plays a decisive role in altering the PF of $BiCuSe_{1-x}Cl_xO$. The PF of pure BiCuSeO is 454 $\mu W\ m^{-1}\ K^{-1}$ at 823 K, and the PF of $BiCuSe_{0.98}Cl_{0.02}O$ is reduced to 222 $\mu W\ m^{-1}\ K^{-1}$ at 773 K.

Figure 5 shows the total thermal conductivity of $BiCuSe_{1-x}Cl_xO$. The thermal conductivity of pure BiCuSeO is lower than that of most oxide-based ceramics, due to the weak bonding energy and low Young's modulus,[16] with thermal conductivity of 0.59 W $m^{-1}\ K^{-1}$ at 873 K. Although the thermal conductivity rises slightly with increasing doping concentration, the thermal conductivity for all samples is around 0.60 W $m^{-1}\ K^{-1}$ at 873 K, and decreases rapidly as the temperature rises. Using the Wiedemann–Franz law, the lattice thermal conductivity of $BiCuSe_{1-x}Cl_xO$ is shown in Fig. 6, from which we can conclude that the total thermal conductivity is dominated by lattice thermal conductivity, with little influence of Cl doping.

As Fig. 7 illustrates, the *ZT* of the Cl-doped BiCuSeO is not higher than that of pure BiCuSeO due to low electrical conductivity. The *ZT* of $BiCuSe_{0.98}Cl_{0.02}O$ is 0.27 at 823 K, while the *ZT* of pure BiCuSeO is 0.65 at 873 K.

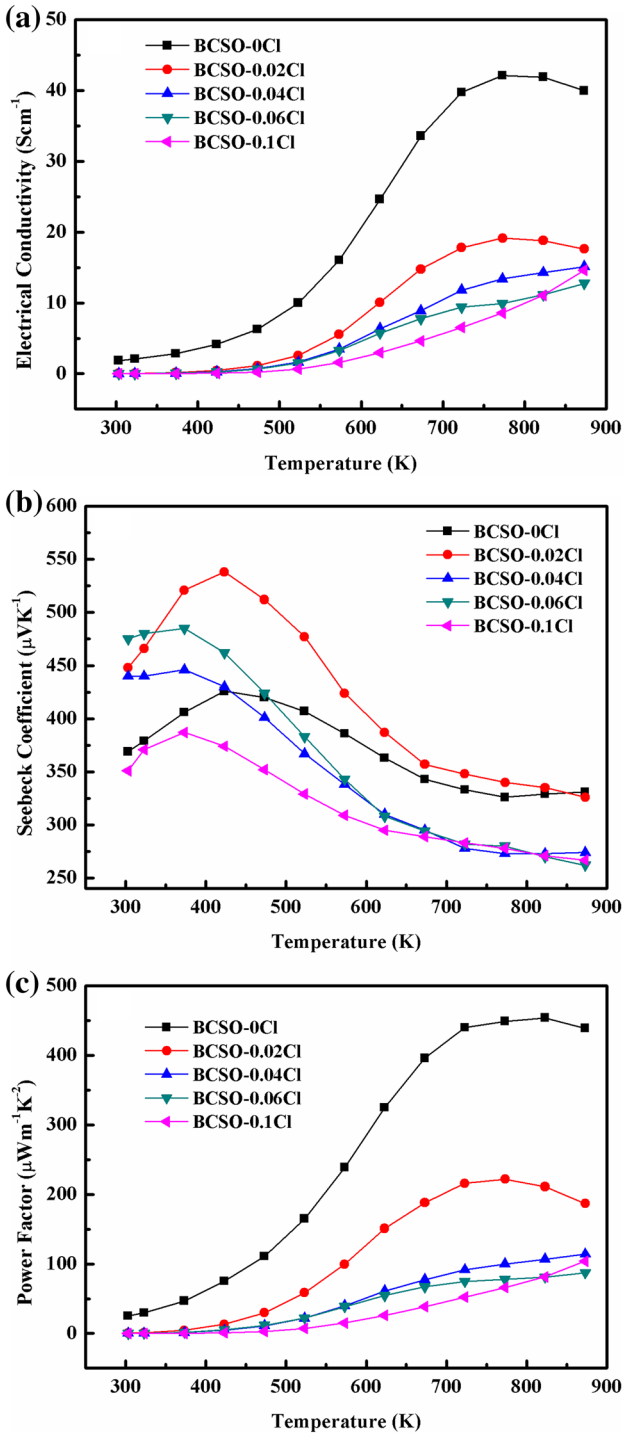

Fig. 4. Electrical properties of $BiCuSe_{1-x}Cl_xO$: (a) electrical conductivity, (b) Seebeck coefficient, (c) power factor.

CONCLUSION

Cl-doped BiCuSeO oxyselenides have been prepared by solid-state reaction combined with SPS. Due to the relatively low doping concentration of Cl, the synthesized samples are still *p*-type semiconductors. The reduction in carrier concentration revealed by Hall measurements proves that Cl^- is successfully doped into the Se site. Although *n*-type BiCuSeO materials were not realized in this work,

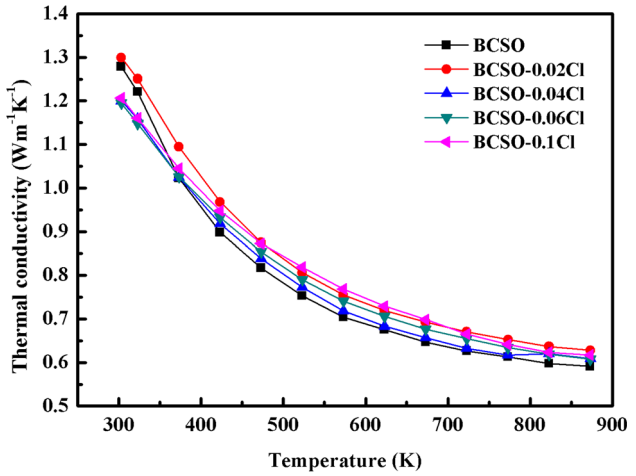

Fig. 5. Thermal conductivity of $BiCuSe_{1-x}Cl_xO$ as a function of temperature.

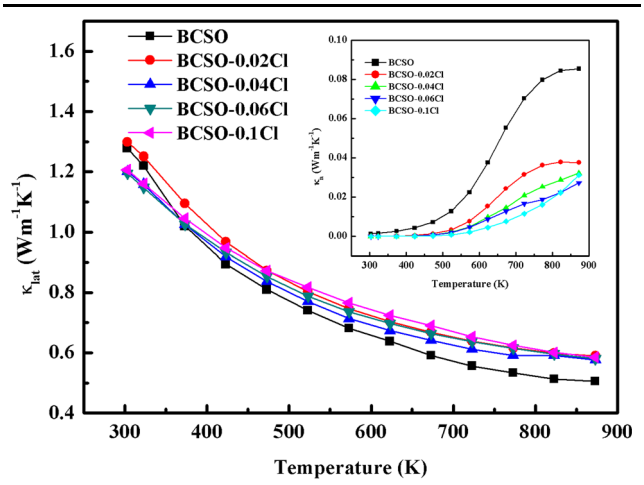

Fig. 6. Lattice thermal conductivity of $BiCuSe_{1-x}Cl_xO$ as a function of temperature. Inset shows carrier thermal conductivity.

Table I. Carrier concentration and mobility of $BiCuSe_{1-x}Cl_xO$

	$x = 0$	$x = 0.02$	$x = 0.04$	$x = 0.06$	$x = 0.1$
Carrier concentration (cm^{-3})	4.82×10^{18}	1.56×10^{16}	8.70×10^{15}	1.31×10^{15}	4.52×10^{15}
Mobility ($cm^2\ V^{-1}\ s^{-1}$)	7.38	4.79	2.26	19.72	1.99

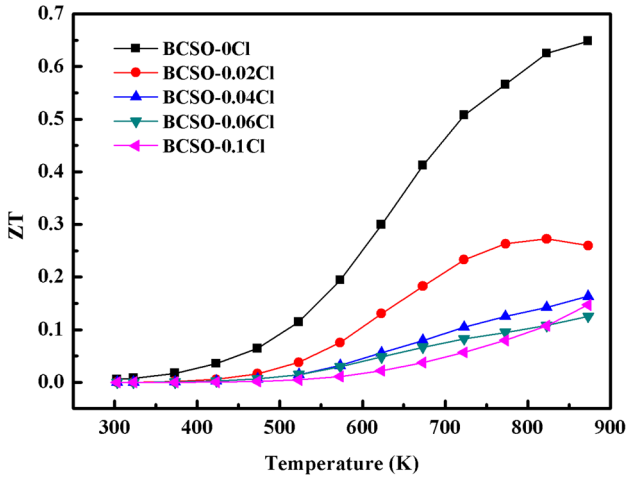

Fig. 7. ZT of $BiCuSe_{1-x}Cl_xO$ as a function of temperature.

high concentrations of Cl or doping with other elements may hold promise for exploring *n*-type BiCuSeO materials.

ACKNOWLEDGEMENTS

This work was financially supported by the National Key Research Program of China under Grant No. 2016YFA0201003, the Ministry of Science and Technology of China through a 973 Program project under Grant No. 2013CB632506, and the National Science Foundation (NSF) of China (51272121, 51328203, 51532003 and 51672155).

REFERENCES

1. G.J. Snyder and E.S. Toberer, *Nat. Mater.* 7, 105 (2008).
2. K. Nielsch, J. Bachmann, J. Kimling, and H. Böttner, *Adv. Energy Mater.* 1, 713 (2011).
3. M.G. Kanatzidis, *Chem. Mater.* 22, 648 (2010).
4. J.P. Heremans, V. Jovovic, E.S. Toberer, A. Saramat, K. Kurosaki, A. Charoenphakdee, S. Yamanaka, and G.J. Snyder, *Science* 321, 554 (2008).
5. L.D. Hicks, T.C. Harman, X. Sun, and M.S. Dresselhaus, *Phys. Rev. B: Condens. Matter* 53, R10493 (1996).
6. J.P. Heremans, C.M. Thrush, and D.T. Morelli, *Phys. Rev. B Condens. Matter Mater. Phys.* 70, 2516 (2004).
7. K. Biswas, J. He, I.D. Blum, C.I. Wu, T.P. Hogan, D.N. Seidman, V.P. Dravid, and M.G. Kanatzidis, *Nature* 189, 414 (2012).
8. J.Q. He, M.G. Kanatzidis, and V.P. Dravid, *Mater. Today* 16, 166 (2013).
9. J. Lan, Y.H. Lin, H. Fang, A. Mei, C.W. Nan, Y. Liu, S. Xu, and M. Peters, *J. Am. Ceram. Soc.* 93, 2121 (2010).
10. T. Tsubota, M. Ohtaki, K. Eguchi, and H. Arai, *J. Mater. Chem.* 7, 85 (1997).
11. T. Okuda, K. Nakanishi, S. Miyasaka, and Y. Tokura, *Phys. Rev. B.* 63, 113104 (2001).
12. L.D. Zhao, D. Berardan, Y.L. Pei, C. Byl, L. Pinsard-Gaudart, and N. Dragoe, *Appl. Phys. Lett.* 97, 092118 (2010).
13. L.D. Zhao, J.Q. He, D. Berardan, Y.H. Lin, J.F. Li, C.W. Nan, and N. Dragoe, *Energy Environ. Sci.* 7, 2900 (2014).
14. J. Li, J.H. Sui, Y.L. Pei, C. Barreteau, D. Berardan, N. Dragoe, W. Cai, J.Q. He, and L.D. Zhao, *Energy Environ. Sci.* 5, 8543 (2012).
15. J. Li, J.H. Sui, C. Barreteau, D. Berardan, N. Dragoe, W. Cai, Y.L. Pei, and L.D. Zhao, *J. Alloys Compd.* 551, 649 (2013).
16. Y.L. Pei, J.Q. He, J.F. Li, F. Li, Q.J. Liu, W. Pan, C. Barreteau, D. Berardan, N. Dragoe, and L.D. Zhao, *NPG Asia Mater.* 5, e47 (2013).
17. L. Pan, D. Berardan, L.D. Zhao, C. Barreteau, and N. Dragoe, *Appl. Phys. Lett.* 102, 023902 (2013).
18. J. Li, J.H. Sui, Y.L. Pei, X.F. Meng, D. Berardan, N. Dragoe, W. Cai, and L.D. Zhao, *J. Mater. Chem. A* 2, 4903 (2014).
19. Y. Liu, L.D. Zhao, Y.C. Liu, J.L. Lan, W. Xu, F. Li, B.P. Zhang, D. Berardan, N. Dragoe, Y.H. Lin, C.W. Nan, J.F. Li, and H.M. Zhu, *J. Am. Chem. Soc.* 133, 20112 (2011).
20. J.H. Sui, J. Li, J.Q. He, Y.L. Pei, D. Berardan, H.J. Wu, N. Dragoe, W. Cai, and L.D. Zhao, *Energy Environ. Sci.* 6, 2916 (2013).
21. J.M. Yang, G. Yang, G.B. Zhang, and Y.X. Wang, *J. Mater. Chem. A* 2, 13923 (2014).